J. Eur. Opt. Society-Rapid Publ. 2026, **22**, 33
© The Author(s), published by EDP Sciences, 2026
https://doi.org/10.1051/jeos/2026036
Available online at: https://jeos.edpsciences.org

**Journal of the European Optical Society-Rapid Publications**

EOSAM 2025
Guest editors: Omar El Gawhary, Stefan Witte, Ignacio Moreno

RESEARCH ARTICLE　　OPEN ACCESS

# Atomic layer deposition for hafnium oxide-based meta-optics in the ultraviolet spectral range

Thomas Siefke[1,2,3,*], Kristin Gerold[1,2], Svetlana Shestaeva[2], Pallabi Paul[1,2], Shawon Alam[4], Daniel Franta[5], Adriana Szeghalmi[1,2], Sven Schröder[2], and Stefanie Kroker[6,7,8]

[1] Friedrich-Schiller-University, Institute of Applied Physics, Albert-Einstein-Strasse 15, 07745 Jena, Germany
[2] Fraunhofer Institute for Applied Optics and Precision Engineering IOF, Albert-Einstein-Str. 7, 07745 Jena, Germany
[3] Ernst-Abbe-Hochschule Jena, University of Applied Sciences, Carl-Zeiss-Promenade 2, 07745 Jena, Germany
[4] Karlsruhe Institute of Technology (KIT), Kaiserstraße 12, 76131 Karlsruhe, Germany
[5] Department of Plasma Physics and Technology, Faculty of Science, Masaryk University, Kotlářská 2, 61137 Brno, Czechia
[6] TU Braunschweig, Institute of Semiconductor Technology, Hans-Sommer-Str. 66, 38106 Braunschweig, Germany
[7] TU Braunschweig, LENA Laboratory for Emerging Nanometrology, Langer Kamp 6a/b, 38106 Braunschweig, Germany
[8] Physikalisch-Technische Bundesanstalt, Bundesallee 100, 38116 Braunschweig, Germany

Received 30 January 2026 / Accepted 4 April 2026

**Abstract.** Hafnium oxide ($HfO_2$) is a high-index dielectric material of growing importance for optical coatings and meta-optical components operating from the ultraviolet (UV) to the visible spectral range. Its large bandgap, chemical stability, and compatibility with established semiconductor processes make it particularly attractive for applications requiring low absorption and precise thickness control. In this work, we investigate the optical material properties of $HfO_2$ thin films deposited by plasma-enhanced atomic layer deposition (PEALD). The complex refractive index is experimentally determined over a broad spectral range extending from the vacuum ultraviolet (140 nm) to the visible (600 nm) by combining spectroscopic ellipsometry, spectrophotometry, and infrared ellipsometry. A comprehensive dispersion model is employed to extract consistent optical constants and thickness values. The results highlight the suitability of PEALD-grown $HfO_2$ films for advanced optical and meta-optical applications.

**Keywords:** Hafniumoxide, meta-optics, ultra violet, refractive index, atomic layer deposition.

## 1 Introduction

Hafnium oxide ($HfO_2$) has attracted significant attention over the past two decades as a functional material in both microelectronics and photonics. In microelectronic devices, $HfO_2$ is well established as a high-permittivity (high-$k$) dielectric replacing $SiO_2$ in advanced metal-oxide-semiconductor field-effect transistors [1–3]. Beyond its electronic functionality, the optical properties of $HfO_2$, namely its high refractive index, wide optical bandgap, and high transparency from the ultraviolet to the infrared, render it attractive for optical coatings, interference filters, and dielectric metasurfaces [4–7]. In particular, the demand for optical components such as wire grid polarizer [8, 9], meta lenses [10] or diffractive optical elements [11] or grating couplers in photonic integrated circuits [12] operating in the ultraviolet and vacuum ultraviolet spectral ranges has increased substantially due to applications in spectroscopy – especially in quantum technologies [13–15] – space optics, and high-resolution microscopy. For these applications, materials must combine low optical absorption with high refractive index contrast and excellent environmental stability. $HfO_2$ fulfills these requirements and offers superior laser-induced damage threshold (LIDT) [16, 17] as well as resistance to radiation-induced damage [18, 19] and chemical degradation and corrosion compared to many alternative high-index oxides. A large variety of deposition techniques have been employed for $HfO_2$ thin films, such as electron beam evaporation [20, 21], magnetron sputtering [22], ion beam sputtering [23, 24], sol-gel [25–27] and atomic layer deposition (ALD) [28–33]. Among these, ALD is particularly suitable for the fabrication of $HfO_2$ thin films with precisely controlled thickness and excellent structural conformality. The self-limiting surface reactions inherent to ALD enables uniform coatings on both planar as well as three-dimensional nanostructured substrates, which is essential for emerging meta-optical concepts relying on subwavelength structuring.

* Corresponding author: thomas.siefke@uni-jena.de

This is an Open Access article distributed under the terms of the Creative Commons Attribution License (https://creativecommons.org/licenses/by/4.0), which permits unrestricted use, distribution, and reproduction in any medium, provided the original work is properly cited.

Numerous studies have been reported on the optical and structural properties of ALD-grown $HfO_2$, demonstrating its applicability in optical thin films across a wide spectra range, for instance as anti-reflection coatings at 266 nm, 355 nm, 532 nm and/or 1064 nm [31, 33], or as high-reflective mirrors at 355 nm and 532 nm [32]. Nevertheless, comprehensive experimental data on its optical constants over an extended spectral range, particularly toward the vacuum ultraviolet (VUV) remain comparatively scarce.

The present work aims to expand the accessible optical database by providing detailed optical properties of PEALD $HfO_2$ thin films down to a wavelength of 140 nm. By combining multiple complementary measurement techniques [34, 35], we extract reliable optical constants from the visible to the VUV range. The resulting dataset provides a solid foundation for the optical design and simulation of $HfO_2$-based coatings and meta-optical devices.

## 2 Thin film deposition

Hafnium oxide thin films are commonly deposited by atomic layer deposition using a variety of hafnium precursor chemistries in combination with either thermal or plasma-assisted oxidation steps. In thermal ALD, both inorganic precursors such as hafnium tetrachloride ($HfCl_4$) [36] and metal-organic precursors tetrakis(dimethylamido) hafnium (TDMAH), tetrakis(ethylmethylamido)hafnium (TEMAH) [37], or β-diketonate-based [38, 39] compounds have been widely employed together with water as the oxidant. While $HfCl_4$-based processes typically require higher deposition temperatures and may lead to halogen-related impurities, metal-organic precursors enable lower-temperature growth and improved process flexibility. In plasma-enhanced ALD (PEALD), the molecular oxidant is replaced by an oxygen plasma, which enhances ligand removal and film densification [40]. PEALD processes using TDMAH or TEMAH have been shown to produce dense, stoichiometric $HfO_2$ films with reduced impurity content at comparatively low substrate temperatures [30–32], making them especially attractive for optical coatings and nanophotonic applications.

Depending on the chosen precursor chemistry and oxidation scheme, the resulting films may exhibit significant differences in growth per cycle, density, impurity concentration, and ultimately optical material properties. The $HfO_2$ thin films investigated in this study were deposited at 100 °C using plasma-enhanced atomic layer deposition in an OpAL reactor (Oxford Instruments Plasma Technology). Tetrakis(dimethylamido)hafnium (TDMAH, $Hf[N(CH_3)_2]_4$) served as the metal precursor, while an oxygen plasma was employed as the oxidizing reactant. Each ALD cycle consisted of a TDMAH precursor pulse (0.4 s), followed by a purge (8 s) and pump-down (2 s) sequence to remove excess precursor and by-products, a gas stabilization period (3 s) followed by an oxygen plasma exposure (10 s) and a final purge (10 s). The details are summarized in Table 1.

The deposition was performed on fused silica substrates in order to enable transmission measurements over a wide spectral range. To ensure sufficient optical sensitivity in ellipsometry measurements while maintaining negligible interference from the substrate backside, a total film thickness of approximately 200 nm was targeted. The deposition process yielded smooth, homogeneous films with excellent macroscopic uniformity.

**Table 1.** ALD parameter for Hafnia deposition using TDMAH and oxygen plasma in an OPAL-tool.

| Step | Parameter | Value |
|---|---|---|
| 1 | TDMAH pulse time | 0.4 s |
| 2 | Purge time | 8 s |
| 3 | Pump down time | 2 s |
| 4 | Gas stabilization time | 3 s |
| 5 | Oxygen plasma pulse | |
| | Time | 10 s |
| | Flow | 50 sccm |
| | Power | 300 W |
| 6 | Purge time | 10 s |

## 3 Optical characterization methods

The optical properties of the $HfO_2$ films were characterized using a combination of spectroscopic ellipsometry and spectrophotometry to cover a broad spectral range. Vacuum ultraviolet and ultraviolet ellipsometric measurements were performed using a Jobin Yvon UVISEL2 ellipsometer at photon energies ranging from 1.5 to 8.7 eV at a fixed angle of incidence of 70°. Additional ellipsometric data in the range from 0.6 to 6.5 eV were acquired with a Jobin Yvon UVISEL ellipsometer using multiple angles of incidence between 55° and 75°. Infrared ellipsometry measurements covering the range from 300 to 6500 $cm^{-1}$ were conducted using a Woollam IR-VASE ellipsometer, again employing variable angles of incidence. Complementary transmission and reflection spectra were recorded using a Perkin Elmer Lambda 1050 spectrophotometer and a Bruker Vertex 80v Fourier-transform infrared spectrometer. For reflectance measurements, illumination from both the film and substrate side was used to enhance sensitivity to interface effects. The experimental data were analyzed using the universal dispersion model implemented in the newAD2 software package [34]. All relevant parameters, including film thickness, dispersion coefficients, and interface roughness, were treated as free fitting parameters. This approach ensured a consistent description of the optical response across all spectral regions and measurement techniques.

## 4 Results and discussion

The combined optical analysis yielded film thickness values between 217 and 221 nm, depending on the specific measurement configuration and spot size. This small variation indicates a high degree of thickness uniformity across the

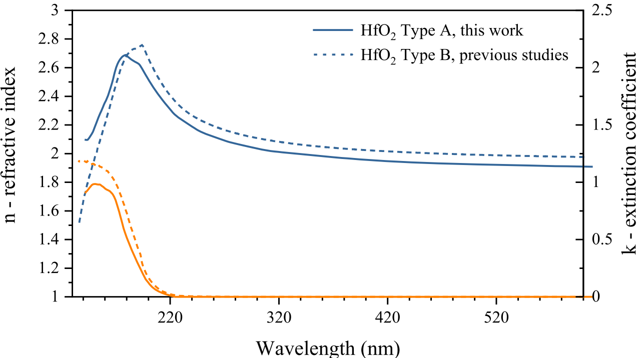


**Fig. 1.** Wavelength dependence of the refractive index of the fabricated hafnia thin films.

**Table 2.** Compared HfO2 thins films prepared by PEALD with different ALD tools.

| | $HfO_2$ – Type A | $HfO_2$ – Type B |
|---|---|---|
| reference | this work; [29] | [33] |
| PEALD tool | OpAL | SILAYO-ICP330 |
| precursors | TDMAH + $O_2$ plasma | TDMAH + $O_2$ plasma |
| substrate temperature | 100 °C | 100 °C |
| density | 7.90 gcm-3 | 8.25 gcm-3 |
| surface roughness | 0.8 nm (XRR) | 1.07 nm (AFM) |

sample. The surface roughness of the top interface was determined to be approximately 1.51 nm (root mean square), with an autocorrelation length of about 5.3 nm. These values correspond to dense, smooth oxide layers produced with PEALD and are comparable to $HfO_2$ thin films on silicon reference samples deposited under similar conditions with 0.8 nm rms (XRR) [29]. The low surface roughness is critical for optical applications, as elevated topography would introduce scatter losses and degrade coating performance in the ultraviolet spectral range.

To evaluate film quality and optical functionality, the extracted refractive index was compared with a previous PEALD-$HfO_2$ study. The thin film examined in this work is designated Type A, while the comparison sample is designated Type B (compare Fig. 1 and Table 2). To minimize the influence of impurity contributions on the optical properties, we compare only processes performed with the same precursor (TDMAH) same oxidizing agent ($O_2$-plasma) and at the same deposition temperature (100 °C), since these are the main parameters affecting carbon and nitrogen levels [30]. The low deposition temperature was chosen to reduce crystallization in the thin films, even though lower temperatures often lead to increased carbon contamination because of incomplete precursor oxidation.

The refractive index of both $HfO_2$ thin films exhibits a pronounced wavelength dependence, with a normal dispersion i.e. high values in the visible and near-ultraviolet spectral range and a gradual decrease toward longer wavelengths. In the ultraviolet region, the refractive index increases significantly as the photon energy approaches the optical band edge, while absorption remains negligible over a wide spectral range down to 230 nm (compare band edge of 5.6 eV [33]). This behaviour is highly advantageous for optical coatings and metasurfaces requiring strong phase modulation with minimal optical losses.

While both $HfO_2$ thin films demonstrate excellent optical properties and comparable transparent regions, Type A and Type B show slight deviations in refractive index. These differences can be attributed to two distinct sources: differences in metrology and deposition conditions.

For Type A thin films, the universal dispersion model (UDM) was employed to extract optical constants [34]. In contrast, optical constants of Type B thin films were extracted from VUV transmittance and reflectance spectra using the Lorentz Calculator (LCalc) [41]. These different analytical methods can introduce systematic deviation, particularly in the VUV region where extinction is dominated by complex inter-band transitions. Nevertheless, both methods are sufficiently mature to provide reliable data and inherently capture the material response, including any influence of i.e. residual impurities.

Typically, different deposition parameters are the main source of such differences. The dominant factor separating the two film types are the different PEALD reactor configuration and associated plasma parameters, which are known to strongly influence $HfO_2$ film density and refractive index [31]. Type A films were deposited using an OpAL PEALD reactor with a remote Inductively Coupled Plasma (ICP) source, while Type B samples were produced on a SILAYO-ICP330 system (Sentech Instruments GmbH), equipped with a direct ICP configuration featuring a Planar Triple Spiral Antenna (PTSA) source. These distinct plasma architectures lead to markedly different energy input and ion bombardment characteristics. The SILAYO PTSA-ICP source delivers higher plasma power density and enhanced ion flux, enabling more effective energetic assistance during film growth. This results in denser films: Type B achieves 8.25 g/cm$^3$ compared to 7.90 g/cm$^3$ for Type A (Table 2). Film density is directly reflected in the refractive index; the denser Type B films exhibit higher n-values across the transparent spectral range. This density-dependent optical property improvement is a well-established phenomenon in oxide thin films and confirms that plasma parameter optimization is a critical control lever for tailoring optical performance in PEALD-$HfO_2$ systems.

X-ray diffraction measurements conducted at the deposition temperature (100 °C) indicate that both Type A and Type B films are X-ray amorphous (not shown here), consistent with low-temperature PEALD processes. However, X-ray amorphous coatings can contain nanocrystalline domains, short-range crystalline order, or point defects that influence optical properties. This may also explain the moderate deviations, especially observed below the absorption edge between the two film sets. The higher density of type B can encourage slight structural rearrangement, such as localized crystallization or structural densification, and affect the absorption profile below the band gap. Despite these structural subtleties, both films maintain low

absorption in the transparent region and preserve well-defined optical bandgaps, indicating that any nanocrystalline or defect-state contributions remain minimal and do not compromise optical performance.

The results of both $HfO_2$ thin films conclusively confirm that PEALD enables the fabrication of optically dense $HfO_2$ layers with properties suitable for advanced optical designs, including applications in ultraviolet meta-optics.

## 5 Conclusion

In summary, we have presented a comprehensive optical characterization of hafnium oxide thin films deposited by plasma-enhanced atomic layer deposition. By combining spectroscopic ellipsometry and spectrophotometry across a wide spectral range, reliable optical constants from the infrared to the vacuum ultraviolet were obtained. The films exhibit high refractive indices, low surface roughness, and excellent optical homogeneity. These findings underscore the suitability of ALD-grown $HfO_2$ for demanding optical applications, particularly in the ultraviolet spectral range and in nanostructured meta-optical systems. The presented dataset provides a valuable reference for optical modeling and design and supports the further development of $HfO_2$-based optical components.

### Funding

The research has been supported by the Deutsche Forschungsgemeinschaft (DFG) (Emmy-Noether-Project SZ253/1-1, 287542364 and Collaborative Research Center (CRC/SFB) 1375), the European Space Agency (ESA) (Contract No. 4000109161/13/NL/RA), under Grant No. 13 N16897 GRADIENT, and BMFTR, Förderprogramm Fusion2040 – Forschung auf dem Weg zum Fusionskraftwerk, FKZ: 13F1009I, SHARP and ATIQ (Fkz: 13N16116), Cluster of excellence QuantumFrontiers (ExC-2123-390837967) as well as from the EMPIR programme 20IND04 ATMOC.

### Conflicts of interest

The authors declare that they have no competing interests to report.

### Data availability statement

The data that support the findings of this study will be made publicly available in the refractiveindex.info database (https://refractiveindex.info/) upon publication.

### Author contribution statement

Thomas Siefke contributed to writing (original draft), formal analysis, funding acquisition, and resources. Kristin Gerold contributed to writing (original draft), visualization, formal analysis, and investigation. Svetlana Shestaeva contributed to writing (review and editing), formal analysis, and investigation. Pallabi Paul contributed to formal analysis, and investigation. Shawon Alam contributed to formal analysis, and investigation. Daniel Franta contributed to formal analysis and investigation. Adriana Szeghalmi contributed to funding acquisition and writing (review and editing). Sven Schröder contributed to writing (review and editing). Stefanie Kroker contributed to funding acquisition and writing (review and editing).

### References

1 Yin YT, Huang CC, Chiu PH, Jiang Y Sen, Hoo JY, Chen MJ, High-quality $HfO_2$ high-K gate dielectrics deposited on highly oriented pyrolytic graphite via enhanced precursor atomic layer seeding, *ACS Appl. Electron. Mater.* **7**, 1943–1952 (2025). https://doi.org/10.1021/ACSAELM.4C02224.

2 Zhang S, Zhang T, Yu H, Li T, Li X, Cui C, et al., Wafer-scale high-κ HfO2 dielectric films with sub-5-Å equivalent oxide thickness for 2D MoS2 transistors, *Nat. Commun.* **17**, 1888 (2026). https://doi.org/10.1038/s41467-026-68584-0.

3 Choi JH, Mao Y, Chang JP, Development of hafnium based high-k materials – A review, *Mater. Sci. Eng. R. Rep.* **72**, 97–136 (2011). https://doi.org/10.1016/J.MSER.2010.12.001.

4 Chow R, Falabella S, Loomis GE, Rainer F, Stolz CJ, Kozlowski MR, Reactive evaporation of low-defect density hafnia, *Appl. Opt.* **32**, 5567 (1993). https://doi.org/10.1364/AO.32.005567.

5 Lehan JP, Mao Y, Bovard BG, Macleod HA, Optical and microstructural properties of hafnium dioxide thin films, *Thin Solid Films* **203**, 227–250 (1991). https://doi.org/10.1016/0040-6090(91)90131-G.

6 Balog M, Schieber M, Michman M, Patai S, Chemical vapor deposition and characterization of HfO2 films from organo-hafnium compounds, *Thin Solid Films* **41**, 247–259 (1977). https://doi.org/10.1016/0040-6090(77)90312-1.

7 Ritala M, Leskelä M, Niinistö L, Prohaska T, Friedbacher G, Grasserbauer M, Development of crystallinity and morphology in hafnium dioxide thin films grown by atomic layer epitaxy, *Thin Solid Films* **250**, 72–80 (1994). https://doi.org/10.1016/0040-6090(94)90168-6.

8 Stock C, Siefke T, Zeitner U, Metasurface-based patterned wave plates for VIS applications, *J Opt Soc Am B* **36**, D97 (2019). https://doi.org/10.1364/JOSAB.36.000D97.

9 Siefke T, Kley E-B, Tünnermann A, Kroker S, Design and fabrication of titanium dioxide wire grid polarizer for the far ultraviolet spectral range, in: *Proceedings of SPIE – The International Society for Optical Engineering*, vol. **9927**, edited by Campo EM, Dobisz EA, Eldada LA (2016). https://doi.org/10.1117/12.2237644.

10 Ossiander M, Meretska ML, Hampel HK, Lim SWD, Knefz N, Jauk T, et al., Extreme ultraviolet metalens by vacuum guiding, *Science* **1979**, 380, 59–63 (2023). https://doi.org/10.1126/SCIENCE.ADG6881.

11 Kaufmann J, Siefke T, Ronning C, Zeitner UD, *Fabrication of EUV gratings via ion irradiation* JW4A.15 (2024).

12 Sorokina A, Meyer AA, Grimpe CF, Du G, Sauer S, Jordan JE, Mehlstäubler TE, Kroker S, Numerical analysis of a high-efficiency dual-material waveguide-grating coupler system for ultraviolet photonics, *Opt. Continuum.* **4**, 10 (2025). https://doi.org/10.1364/OPTCON.568352.

13 Alombert-Goget G, Trichard F, Li H, Pezzani C, Silvestre M, Barthalay N, et al., Titanium distribution profiles obtained by luminescence and LIBS measurements on Ti: Al2O3 grown by Czochralski and Kyropoulos techniques, *Opt. Mater. (Amst)* **65**, 28–32 (2017). https://doi.org/10.1016/J.OPTMAT.2016.09.049.

14 Trichard F, Moncayo S, Devismes D, Pelascini F, Maurelli J, Feugier A, et al., Evaluation of a compact VUV spectrometer

for elemental imaging by laser-induced breakdown spectroscopy: application to mine core characterization, *J. Anal. At. Spectrom.* **32**, 1527–134 (2017). https://doi.org/10.1039/C7JA00185A.

15 Bassel L, Motto-Ros V, Trichard F, Pelascini F, Ammari F, Chapoulie R, et al., Laser-induced breakdown spectroscopy for elemental characterization of calcitic alterations on cave walls, *Environ. Sci. Pollut. Res.* **24**, 2197–2204 (2017). https://doi.org/10.1007/S11356-016-7468-5/FIGURES/5.

16 Alvisi M, Di Giulio M, Marrone SG, Perrone MR, Protopapa ML, Valentini A, et al., HfO2 films with high laser damage threshold, *Thin Solid Films* **358**, 250–258 (2000). https://doi.org/10.1016/S0040-6090(99)00690-2.

17 Stolz CJ, Thomas MD, Griffin AJ, BDS thin film damage competition, **7132**, 107–113 (2008). https://doi.org/10.1117/12.806287.

18 Fan Y, Liu J, Jiang J, Jiang LM, Ion radiation effects on the stability of hafnium oxide-based ferroelectric thin films: mechanisms and regulation, *IEEE Trans. Device Mater. Rel.* **25**, 314–322 (2025). https://doi.org/10.1109/TDMR.2025. 3550950.

19 Ding M, Liu X, Damage effect of hafnium oxide gate dielectric based metal-oxide-semiconductor structure under gamma-ray irradiation, *AIP Adv.* **11**, 65304 (2021). https://doi.org/10.1063/5.0048080/993914.

20 Kant S, Kumari N, Kumar M, Effect of deposition conditions on the morphological, optical, and corrosion behavior of electron beam evaporated high-performance HfO2 thin films, *Appl. Phys. A Mater. Sci. Process.* **131**, 631 (2025). https://doi.org/10.1007/s00339-025-08755-w.

21 Ramzan M, Rana AM, Ahmed E, Bhatti AS, Hafeez M, Ali A, et al., Optical description of HfO2/Al/HfO2 multilayer thin film devices, *Curr. Appl. Phys.* **14**, 1854–1860 (2014). https://doi.org/10.1016/J.CAP.2014.10.023.

22 Araiza J de J, Álvarez-Fraga L, Gago R, Sánchez O, Surface morphology and optical properties of hafnium oxide thin films produced by magnetron sputtering, *Materials* **16**, 5331 (2023) https://doi.org/10.3390/MA16155331.

23 Thielsch R, Gatto A, Kaiser N, Mechanical stress and thermal-elastic properties of oxide coatings for use in the deep-ultraviolet spectral region, *Appl. Opt.* **41**, 16 (2002) https://doi.org/10.1364/AO.41.003211.

24 Bundesmann C, Neumann H, Tutorial: The systematics of ion beam sputtering for deposition of thin films with tailored properties, *J. Appl. Phys.* **124**, 231102 (2018). https://doi.org/10.1063/1.5054046.

25 Jiang K, Anderson JT, Hoshino K, Li D, Wager JF, Keszler DA, Low-energy path to dense $HfO_2$ thin films with aqueous precursor, *Chem. Mater.* **23** (4), 945–952 (2011). https://doi.org/10.1021/cm102082j.

26 Nishide T, Honda S, Matsuura M, Ide M, Surface, structural and optical properties of sol-gel derived $HfO_2$ films, *Thin Solid Films* **371**, 61 (2000) https://doi.org/10.1016/S0040-6090(00)01010-5.

27 Zaharescu M, Teodorescu VS, Gartner M, Blanchin, MG, Barau A, Anastasescu M, Correlation between the method of preparation and the properties of the sol–gel $HfO_2$ thin films, *J. Non-Cryst. Solids* **354**, 409 (2008) https://doi.org/10.1016/j.jnoncrysol.2007.07.097.

28 Kull M, Piirsoo HM, Tarre A, Mändar H, Tamm A, Jõgiaas T, Hardness, modulus, and refractive index of plasma-assisted atomic-layer-deposited hafnium oxide thin films doped with aluminum oxide, *Nanomaterials* **13**, 1607 (2023). https://doi.org/10.3390/NANO13101607/S1.

29 Shestaeva S, Bingel A, Munzert P, Ghazaryan L, Patzig P, Tünnermann A, Szeghalmi A, Mechanical, structural, and optical properties of PEALD metallic oxides for optical applications, *Appl. Opt.* **56**, 4 (2017) https://doi.org/10.1364/AO.56.000C47.

30 Kim K-M, Jang JS, Yoon S-G, Yun J-Y, Chung N-K, Structural, optical and electrical properties of $HfO_2$ thin films deposited at low-temperature using plasma-enhanced atomic layer deposition, *Materials* **13**(9), 2008 (2020). https://doi.org/10.3390/ma13092008.

31 Lapteva M, Beladiya V, Riese S, Hanke P, Otto F, Fritz T, Schmitt P, Olaf Stenzel O, Andreas Tünnermann A, Szeghalmi A, Influence of temperature and plasma parameters on the properties of PEALD $HfO_2$, *Opt. Mater. Express* **11**, 1918–1942 (2021). https://doi.org/10.1364/OME.422156.

32 Beladiya V, Faraz T, Schmitt P, Munser AS, Schröder S, Riese S, Mühlig C, Schachtler D, Steger F, Botha R, Otto F, Fritz T, Helvoirt C, Kessels WMM, Gargouri H, Szeghalmi A, Plasma-enhanced atomic layer deposition of $HfO_2$ with substrate biasing: thin films for high-reflective mirrors, *ACS Appl. Mater. Interfaces* **14**, 14677−14692 (2022). https://doi.org/10.1021/acsami.1c21889.

33 Alam S, Paul P, Beladiya V, Schmitt P, Stenzel O, Trost M, Wilbrandt S, Mühlig C, Schröder S, Matthäus G, et al., Heterostructure Films of $SiO_2$ and $HfO_2$ for High-Power Laser Optics Prepared by Plasma-Enhanced Atomic Layer Deposition, *Coatings* **13**, 278 (2023). https://doi.org/10.3390/coatings13020278.

34 Franta D, Nečas D, Ohlídal I, Universal dispersion model for characterization of optical thin films over a wide spectral range: application to hafnia, *Appl. Opt.* **54**, 9108 (2015). https://doi.org/10.1364/AO.54.009108.

35 Siefke T, Kroker S, Pfeiffer K, Puffky O, Dietrich K, Franta D, et al., Materials Pushing the Application Limits of Wire Grid Polarizers further into the Deep Ultraviolet Spectral Range, *Adv. Opt. Mater.* **4**, 1780–1786 (2016). https://doi.org/10.1002/adom.201600250.

36 Puurunen RL, Analysis of hydroxyl group controlled atomic layer deposition of hafnium dioxide from hafnium tetrachloride and water, *J. Appl. Phys.* **95**, 4777–4786 (2004). https://doi.org/10.1063/1.1689732.

37 Triyoso DH, Hegde RI, White BE, Tobin PJ, Physical and electrical characteristics of atomic-layer-deposited hafnium dioxide formed using hafnium tetrachloride and tetrakis (ethylmethylaminohafnium), *J. Appl. Phys.* **97**, 124107 (2005). https://doi.org/10.1063/1.1947389.

38 Pasko SV, Hubert-Pfalzgraf LG, Abrutis A, Richard P, Bartasyte A, Kazlauskiene V, New sterically hindered Hf, Zr and Y β-diketonates as MOCVD precursors for oxide films, *J. Mater. Chem.* **14**, 1245–1251 (2004). https://doi.org/10.1039/B401052C.

39 Zherikova KV, Morozova NB, Zelenina LN, Sysoev SV, Chusova TP, Igumenov IK, Thermal properties of hafnium(IV) and zirconium(IV) β-diketonates, *J. Therm. Anal. Calorim.* **92**, 729–734 (2008). https://doi.org/10.1007/s10973-008-9027-x.

40 Martínez-Puente MA, et al., ALD and PEALD deposition of HfO2 and its effects on the nature of oxygen vacancies, *Mater. Sci. Eng. B* **285**, 115964 (2022). https://doi.org/10.1016/J.MSEB.2022.115964.

41 Stenzel O, Wilbrandt S, Friedrich KF, Kaiser N, Realistische Modellierung der NIR/VIS/UV-optischen Konstanten dünner optischer Schichten im Rahmen des Oszillatormodells, *VIP* **21**, 15–23 (2009). https://doi.org/10.1002/vipr.200900396.